



**HAL**  
open science

# Pulse-reactor core monitoring with an innovative optical neutron detector

Maxime Lamotte, G. de Izarra, C. Jammes

## ► To cite this version:

Maxime Lamotte, G. de Izarra, C. Jammes. Pulse-reactor core monitoring with an innovative optical neutron detector. Nuclear Instruments and Methods in Physics Research Section A: Accelerators, Spectrometers, Detectors and Associated Equipment, 2021, 995, pp.165086. 10.1016/j.nima.2021.165086 . cea-03149071

**HAL Id: cea-03149071**

**<https://cea.hal.science/cea-03149071>**

Submitted on 22 Feb 2021

**HAL** is a multi-disciplinary open access archive for the deposit and dissemination of scientific research documents, whether they are published or not. The documents may come from teaching and research institutions in France or abroad, or from public or private research centers.

L'archive ouverte pluridisciplinaire **HAL**, est destinée au dépôt et à la diffusion de documents scientifiques de niveau recherche, publiés ou non, émanant des établissements d'enseignement et de recherche français ou étrangers, des laboratoires publics ou privés.

# Pulse-reactor core monitoring with an innovative optical neutron detector.

M. LAMOTTE<sup>a</sup>, G. DE IZARRA<sup>a</sup>, C. JAMMES<sup>a</sup>

<sup>a</sup>CEA, DES, IRESNE, DER, Instrumentation Sensors and Dosimetry Laboratory,  
Cadarache,  
F-13108 Saint-Paul-lez-Durance, France.

---

## Abstract

To minimize uncertainty and strengthen estimation of energy deposited during power transients, we set up an online passive neutron flux measurement of a pulse reactor.

Optical fission chambers, are being developed in the framework of dependable neutron flux instrumentation for Sodium-cooled Fast Reactor (SFR) and Molten-Salt Reactor (MSR) of Generation IV by the French Atomic Energy and Alternative Energies Commission (CEA). Neutron interactions with a fissile layer coating release heavy-ions in the MeV-range, eventually leading to spontaneous photon emission in the ultraviolet to infrared range of the surrounding noble gas. Prototypes have previously been tested in an ideal pure neutron field. In this paper, linearity of optical signal versus reactor power is assessed during startups and high power transients up to 21.6 GW. Excellent linearity results are obtained over 5 reactor power decades and detection remain possible over 7 decades. Detection range is only restrained by photodetector properties. Such detector may be routinely employed for high-dynamic transients monitoring by the core caisson of pulse reactors.

*Keywords:* fission chambers, radiation-hard detectors, gaseous detectors, gas scintillation

*PACS:* 29.85.-cAMODIF, 28.50.Dr, 28.41.Rc

---

## 1. Introduction

The French Atomic Energy and Alternative Energies Commission (CEA) proposes a new generation of neutron detectors for the neutron flux monitoring of Sodium-cooled Fast Reactors (SFR) and Molten Salt Reactors (MSR). These detectors are based on the luminescence of rare gases excited by collisions with charged particles [1–3] and spontaneously de-excited, generating discrete emission lines.

Photons in the near-infrared spectrum can be channelled in optical fibre under harsh radiation environment over long distances, as low attenuation in silica fibres [4] have been reported in this region.

Previous work on this detector focused on proof-of-concept achievement, light spectrum analysis, signal strength optimisation and solid-state photodetector assessment in a gamma-free cold-neutron beam.

Linearity of optical signal strength against neutron flux is required for future reactor monitoring systems, we therefore assessed the very same CANOE detector in the pool of CABRI, a high-power transient reactor. This unique experimental facility dedicated to fuel rods failures during power excursions allows testing of instrumentation over 11 decades of reactor power, as found in SFR and MSR.

## 2. Materials and methods

The present section details materials, facilities and methods used for neutron flux measurements by passive optical means on a CANOE (Capteur de Neutrons à Optique Expérimentale) gaseous detector.

### 2.1. Luminescent fission chamber assembly

The CANOE detector initially designed for the very low flux pure neutron field of ORPHÉE reactor, was repurposed and re-configured for linearity assessment. CANOE consists of a 2 mm thick aluminium tube, 30 mm diameter and 80 mm long hosting a 500 nm thin pure  $^{235}\text{U}_3\text{O}_8$  layer deposited on a 18 mm diameter

and 200 $\mu\text{m}$  thick stainless steel disk, pictures on Fig. 1. Noble gas filling of the detector can be performed between 0.5 to 5 atm. As maximal light intensity was obtained under 2 atm of ultra-pure Air Liquide N50 neon during experiments on ORPHÉE neutron beams, an identical filling was set in the detector. A fused silica window, maintained against the detector body by a tapered flange and a silicone o’ring ensures light transmission towards optical fibres and an airtight construction.

Near-infrared emission spectrum was originally seek, as wavelengths between 800 and 1100 nm are less prone to Radiation Induced Absorption (RIA) in standard silica optical fibres [4].

As pointed after 120 h of irradiation on ORPHÉE, resulting in  $4\text{E}14 \text{ n.cm}^2$  fluence deposition, no RIA was detected between 450 nm to 2  $\mu\text{m}$  wavelengths, since the optical fibre was away from radiation fields, allowing lossless visible-spectrum light transmission. To improve the signal to noise ratio, it was decided to fill CANOE with neon. This resulted in strong light emission at 585 nm while argon mainly produced peaks at 750, 763 and 912 nm. Low noise high sensitivity photon counters, as the employed Hamamatsu C13001-01, made of a single cooled silicon Avalanche PhotoDiode in Geiger mode (APD-Geiger), display significantly better detection efficiency in visible wavelengths, from less than 3 % at 900 nm up to 40 % at 585 nm. Hence, using neon as filling gas improved signal-to-noise ratio up to a decade.

The APD-Geiger photon counting module displays a very low dark noise, less than 10 cps, a linearity over 5 decades and a non-destructive saturation after 7 light power decades. As this photon counter has a single 125  $\mu\text{m}$  diameter large photodiode, it doesn’t suffer from Silicon Photomultiplier (SiPM) crosstalk and linearity bias at high count rates, making it suitable for our linearity assessment experiment.

For irradiations on CABRI, we assumed the fluence deposited by several millisecond-long pulses was not high enough to induce significant RIA in silica fibres. We therefore connected the 2-bars neon filled CANOE to three segments of FG200-LEA, 200  $\mu\text{m}$  diameter silica-core optical fibres. All 3 fibres were held loose

on a 2 mm thick plastic string, acting as mechanical fuse. The assembly was ultimately pulled in light-tight heat-shrinkable sleeves, resulting in a custom-made tri-redundant high strength fibre bundle.

## *2.2. Data acquisition system*

Data acquisition was performed on the very same Textronic MSA9104A oscilloscope with 1 billion points memory as used on ORPHÉE reactor [1]. A 125 Msamples/s acquisition allowed 4 seconds long recordings, triggered manually from control room countdown.

We also evaluated a low-cost, small-footprint alternative for narrow TTL pulse counting from the photon detector with Red Pitaya boards.

This system hosts two 14 bits Analogue to Digital Converters (ADC) connected to a FPGA, capable of 125 MSamples/s scans and providing an Ethernet interface, allowing remote operation and configuration.

A Verilog code counted rising edges on a ADC input during a user-settable census period, ranging from 1 ms to 1 second. A C-language routine eventually send buffered value translated into counts per second over Ethernet for direct visualisation, and towards onboard storage for further analysis.

The very particular CABRI reactor operation forbids human presence in its building after criticality, experimenters have therefore no access to devices but trough an optical fibre high speed Ethernet port located in a remote control room, 500 metres away.

## *2.3. CABRI power pulse reactor*

CABRI is a pool-type experimental reactor dedicated to fuel stress under Reactivity Initiated Accident [8]. CABRI core is made of 6% enrichment  $^{235}\text{UO}_2$  pellets contained in 1487 stainless steel clads. A large test cell, approx. 30 cm diameter, in the middle of the core hosts a PWR fuel rod within a pressurized water loop. CABRI can reach a 23.7 MW steady state power level with active cooling, or 100 kW if relaying solely on natural convection. Reactivity control is

ensured by a set of 6 control and safety rods, each made of 23 hafnium pins [9]. CABRI features a reactivity injection system based on fast depressurization of  $^3\text{He}$  (a strong neutron absorber) contained in 96 tubes located among CABRI fuel rods. Fast depressurization, from 14.85 atm to vacuum, of  $^3\text{He}$  induces a reactivity increase of about 4\$ within tens of milliseconds. CABRI power can burst from 100 kW up to 21.6 GW in few ms and decreases with a similar dynamic thanks to Doppler effect in the fuel and other negative feedbacks.

Reactor power monitoring is performed by 2 boron-lined gamma-compensated ionisation chambers for reactor control connected to a low sampling-rate current measurement system in all phases but power transient (hereafter referred at HN1 and HN2). 5 high-speed neutron measurement systems are dedicated to power transient analysis, each has its detector being placed at different distances from the core to precisely monitor an assigned power range [13]. All detectors are placed behind a 15 cm thick lead shield to attenuate gamma-induced ionisation currents.

CANOE was placed in an experimental box of the size of CABRI fuel assemblies, approximately 8.6 cm by 8.6 cm, 1.2 m long. This waterproof aluminium lead-weighted box is used during commissioning tests [12], holding standard fission chambers CFUL01 and a set of dosimeters, at steady reactor power of 5 kW. It features a 30 mm diameter 20 m long polymer pipe for cable placement. Pictures of CANOE being placed in this experimental box are presented on Fig. 1

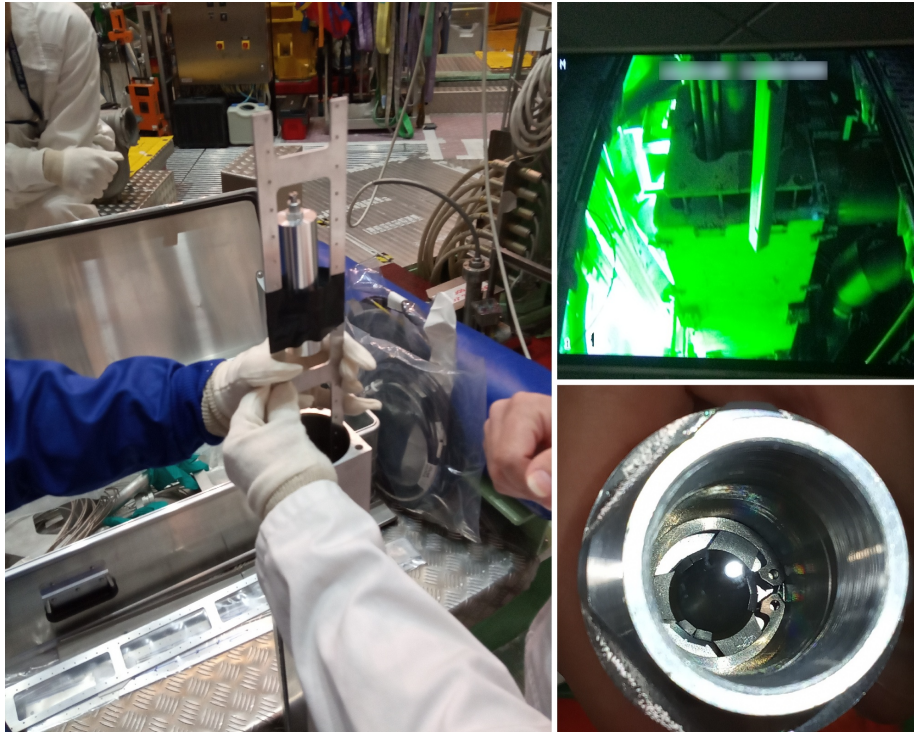


Figure 1: Left: placement of CANOE inside the experimental box.  
Up: immersion of the experimental box in CABRI pool, by the core caisson.  
Down: close-up view of CANOE 0.5  $\mu\text{m}$  thick fissile layer, as seen through its silica window.

The box was immersed in reactor pool, by the core caisson. A neutron/gamma field with a neutron flux of  $1.37\text{E}12 \text{ n.cm}^2.\text{s}^{-1}$ , 90 % thermalized below Cadmium energy cut-off, and a gamma dose of 350 Gy/h is expected at 1 MW reactor power at this location. A drawing of CABRI pool is presented Fig. 2.

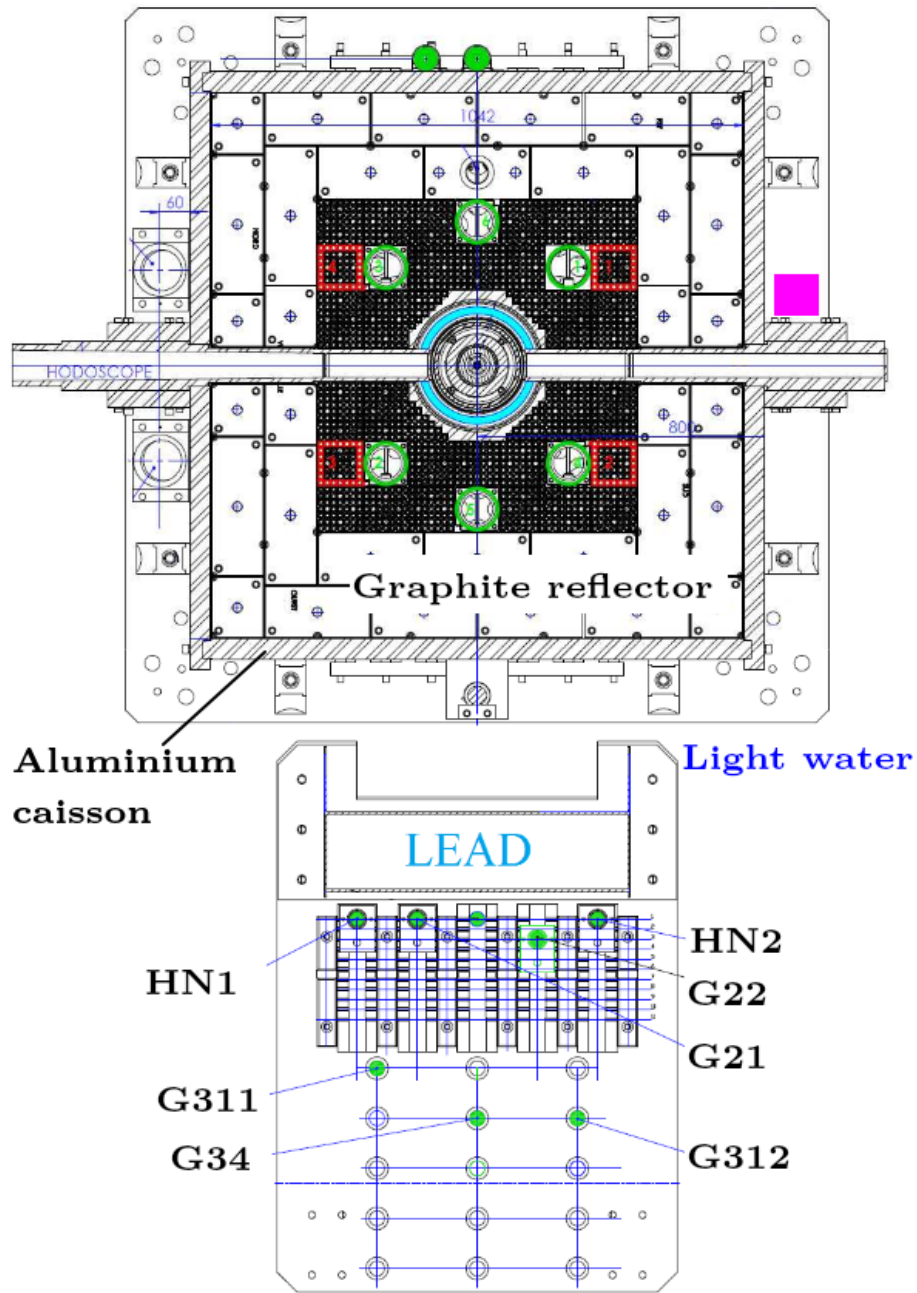


Figure 2: View of CABRI reactor pool. CANOE experimental box is placed on the magenta square, by core caisson. 5 pulses monitoring and 2 reactor control boron chambers are placed behind 15 cm of lead and 30 cm of light water. Green circles emphasise safety and control rods, red squares represent  $^3\text{He}$  tubes. Central structure contains a pressurized water loop a section of PWR rod, monitored by the lateral hodoscope.

Prior our experiment, no fission chambers have ever been placed by the core during a power pulse as a 21.6 GW pulse would require a destructive 500 W power transmission inside standard CFUL01 chambers. Placement of a neutron detector by the core during a pulse reduces uncertainties due to thermal neutron transport in water.

### **3. Results**

Prior each CABRI power pulse, startups up to 100 kW lasting tens of seconds allows for estimation of the detection limit of CANOE, translated into incident neutron flux. Steady power was maintained for as long as 10 minutes for safety systems to be checked before a power pulse.

Neutron monitoring systems HN1 and HN2 having a detection limit of 300 mW reactor power, 6 power decades can be assessed on CANOE during reactor startup. Power pulses extend this range up to 11 decades.

#### *3.1. Reactor startups*

Upon switching on the photon counter, a 104 cps stray signal was observed, due to room light input in the optical fibre or detector enclosure.

Reactor startup neutron flux acquired with a CANOE detector are presented along HN1 and HN2 traces on Fig. 3. A detection limit of 300 W was found on CANOE, corresponding to a neutron flux of about  $4E8 \text{ n.cm}^2.\text{s}^{-1}$ .

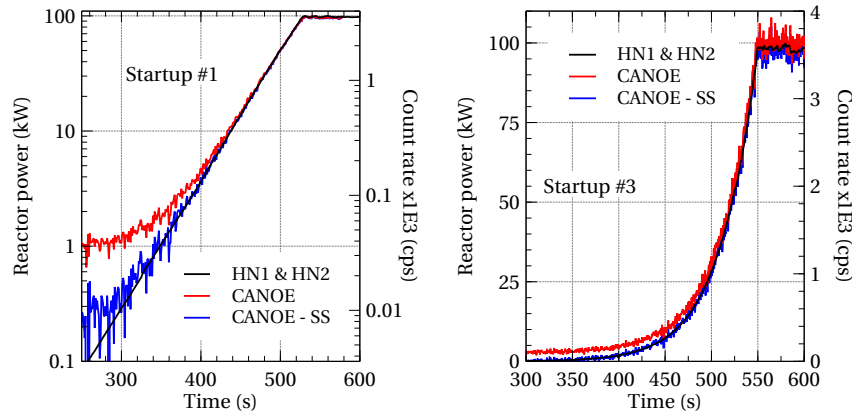


Figure 3: CABRI reactor startup, as recorded by ionisation chambers HN1 and HN2 monitored in current mode, and CANOE.  
 Left: 100 ms sampling re-sampled to 1 second during startup number 1. SS: correction of Stray Signal.  
 Right: 400 ms sampling during startup number 3, shown on a logarithmic scale to observe the CANOE detection limit.

HN1 and HN2 boron-lined chambers were exploited on their mean current output while the photo-detector converts CANOE light into discrete TTL pulses. As a result, more fluctuations were observed at low reactor power on CANOE, as it would be on any standard fission chamber used in pulse mode. Sampling rates ranged between 100 to 400 ms during the 4 reactor startups monitored with luminescent fission chambers. One can notice the good agreement between boron-lined chambers and CANOE scintillation strength over 3 reactor power decades. At 100 kW power, a 3600 cps CANOE count rate was measured.

### 3.2. Reactor pulses

Three CABRI pulses have been produced during a single morning, as a commissioning campaign prior to PWR fuel-rod transient power stress test. Tab. 1 sums-up the pulses endured by CANOE. The very high power surge rate of CABRI —up to a decade per millisecond— forbids any re-setting of our readout system, lacking fast automatic scaling routine. To avoid a buffer overflow of the Red Pitaya FPGA and to obtain detailed profiles of reactor pulses, we set-up a 1 ms short sampling time for all readouts,

Pulse	$^3\text{He}$ Pressure (atm)	Peak power (GW)	FWHM (ms)	Energy (J)
1	7	13.6	10.5	177
2	11.3	21.6	8.95	237
3	9	18	9.37	208

Table 1: CANOE monitored CABRI reactor pulses characteristics . FWHM: Full Width at Half Maximum.

our counting program limit.

At 100 kW steady power, 3 to 4 TTL pulses were recorded each millisecond from the photon detector, too few to perform absolute calibration. When high power pulses are produced in CABRI, a post-pulse plateau of several tens of megawatts, visible before safety rods fall, lasts tens of milliseconds. After a 13.6 GW pulse, a 67 MW plateau is expected, where about  $2.41\text{E}+6$  cps are forecasted from the photon detector, still in its linearity region. As a result, the CANOE TTL-pulses frequency to reactor power calibration was applied on the post-pulse plateau, with high-flux-dedicated boron-lined ionisation chamber data G22 and G34. An excellent agreement between standard ionisation chambers and CANOE measurements is reported on the rising edge of the pulse, up to photodetector saturation limit, as shown Fig. 4.

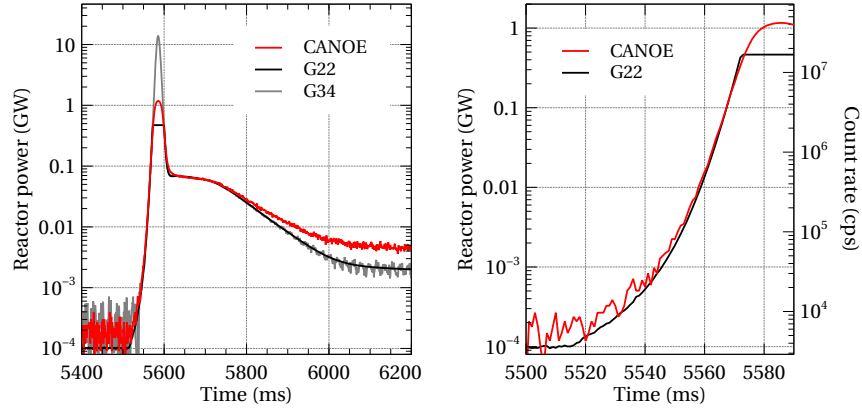


Figure 4: Left: CANOE and reference ionisation chamber traces during the first 13.6 GW pulse. Count rate is for CANOE trace. Right: closeup of the first monitored power pulse, deviation of CANOE signal linearity is visible from  $4\text{E}+6$  cps and photodetector saturation occurs at  $4\text{E}+7$  cps or 1.1 GW reactor power. Reference ionisation chamber G22 routinely saturates at 465 MW.

Above 110 MW, a deviation of CANOE signal with other neutron flux monitors is reported, corresponding to an approximately  $4\text{E}+6$  cps TTL pulses from the photon detector, where its documented linearity begins to deviate. At this point, a software correction of APD's dead-time remains possible. Even though, saturation is visible at 1.1 GW, or about  $4\text{E}+7$  cps, higher than the C13001-01 manufacturer claimed maximum,  $3\text{E}+7$  cps.

A post-pulse remanent signal, not due to control-rods drop time, is visible solely on CANOE traces for several minutes. CANOE high aluminium content — about 120g— may induce a significant activation, not experienced by other detectors located tens of centimetres away from the core, behind lead shielding. General radioactive decay law shape and disappearance of the remanent CANOE signal after 11 minutes, about 5  $^{28}\text{Al}$  half-lives (2.2 minutes) points a possible main contribution of neutron-activated aluminium beta decay to this phenomenon. Fitting an  $^{28}\text{Al}$  decay curve on CANOE post pulses traces, normalized to initial count rates, showed a nearly perfect superposition. Such post-pulse signal can be attenuated by relying on envelope material producing long-lived activation products such as steel, Zircalloy or Inconel.

#### 4. Conclusion

An on-line passive neutron detector based on gas scintillation has been assessed during reactor startups and power pulses.

Linearity of the CANOE detector response as a function of neutron flux was found to be comparable to standard ionisation chambers, over 5 decades.

The employed photodetector dynamic range limits power monitoring over 7 decades, relying solely on photoelectric pulses counting.

The weak post-pulse signal found on a CANOE detector is likely induced by aluminium structure activation, a behaviour to be limited on future designs based on other alloys body parts.

Future experiments with CANOE detectors will focus on lowering the detection limit with optical assemblies and assessment of wide range photodiodes.

#### 5. Acknowledgments

The authors are very thankful to the CABRI staff and more particularly to V.Cano for his trustiness during this exceptional experiment; E.Gohier, J.Lecerf and A.Gruel for their technical support.

#### References

- [1] M. Lamotte, G. De Izarra, C. Jammes, Design and irradiation test of an innovative optical ionization chamber technology, Nuclear Instruments and Methods in Physics Research Section A: Accelerators, Spectrometers, Detectors and Associated Equipment (2020) 163945.
- [2] M. Lamotte, G. de Izarra, C. Jammes, Development and first use of an experimental device for fission-induced spectrometry applied to neutron flux monitoring, Nucl. Instrum. Methods Phys. Res. A (2019) 163236.
- [3] M. Lamotte, G. De Izarra, C. Jammes, Heavy-ions induced scintillation experiments, Journal of Instrumentation 14 (09) (2019) C09024.

- [4] Cheymol, Guy and Long, Herve and Villard, Jean Francois and Brichard, Benoit, High level gamma and neutron irradiation of silica optical fibers in CEA OSIRIS nuclear reactor, *IEEE Transactions on Nuclear Science* 55 (4) (2008) 2252–2258.
- [5] J.-P. Hudelot, E. Fontanay, C. Molin, A. Moreau, L. Pantera, J. Lecerf, Y. Garnier, B. Duc, Cabri facility upgrade, refurbishment, recommissioning and experimental capacities, in: *PHYSOR 2016: The Physics of Reactors conference*, 2016, pp. ISBN–978.
- [6] J. Lecerf, Y. Garnier, J. Hudelot, B. Duc, L. Pantera, Study of the linearity of Cabri experimental ionization chambers during ria transients, in: *EPJ Web of Conferences*, Vol. 170, EDP Sciences, 2018, p. 04015.
- [7] A. Ferrari, P. R. Sala, A. Fasso, J. Ranft, U. Siegen, et al., Fluka: a multi-particle transport code, Tech. rep., Stanford Linear Accelerator Center (SLAC) (2005).
- [8] AUSY, Modélisation tripoli pour la caractérisation neutronique du réacteur Cabri dans la configuration BEP, Tech. Rep. NT DER/SPRC/LPN /16-1728 ind. 1, CEA - Cadarache (2016).
- [9] AUSY, M. Maillot, Étude neutronique de référence du coeur Cabri dans la configuration boucle à eau pressurisée (BEP), Tech. Rep. NT DER/SPRC/LPN /16-1735 ind. A, CEA - Cadarache (2016).
- [10] J. Lecerf, O. Clamens, Analyse physique des essais C1 et C7 en vue de la caractérisation neutronique du coeur de Cabri, Tech. Rep. SPESI/LP2E/NT/2019-002 ind. A, CEA - Cadarache (2019).
- [11] Vlachoudis, Vasilis et al., FLAIR: a powerful but user friendly graphical interface for FLUKA, in: *Proc. Int. Conf. on Mathematics, Computational Methods & Reactor Physics (M&C 2009)*, vol 1, 2009, pp. 3
- [12] J.-P. Hudelot, E. Fontanay, C. Molin, A. Moreau, L. Pantera, J. Lecerf, Y. Garnier, B. Duc, Cabri facility upgrade, refurbishment, recommissioning

and experimental capacities, in: PHYSOR 2016: The Physics of Reactors conference, 2016, pp. ISBN-978.

- [13] J. Lecerf, Y. Garnier, J. Hudelot, B. Duc, L. Pantera, Study of the linearity of Cabri experimental ionization chambers during ria transients, in: EPJ Web of Conferences, Vol. 170, EDP Sciences, 2018, p. 04015.
- [14] A. Ferrari, P. R. Sala, A. Fasso, J. Ranft, U. Siegen, et al., Fluka: a multi-particle transport code, Tech. rep., Stanford Linear Accelerator Center (SLAC) (2005).